BIOCHEMISTRY
including biophysical chemistry & molecular biology
Article

Biochemistry **2010,** *49,* 1115–1126 1115
DOI: 10.1021/bi902181v

A Novel Method of Production and Biophysical Characterization of the Catalytic Domain of Yeast Oligosaccharyl Transferase[†,‡]

Chengdong Huang, Smita Mohanty,* and Monimoy Banerjee

Department of Chemistry and Biochemistry, Auburn University, Auburn, Alabama 36849

Received September 9, 2009; Revised Manuscript Received December 31, 2009

ABSTRACT: Oligosaccharyl transferase (OT) is a multisubunit enzyme that catalyzes N-linked glycosylation of nascent polypeptides in the lumen of the endoplasmic reticulum. In the case of *Saccharomyces cerevisiae*, OT is composed of nine integral membrane protein subunits. Defects in N-linked glycosylation cause a series of disorders known as congenital disorders of glycosylation (CDG). The C-terminal domain of the Stt3p subunit has been reported to contain the acceptor protein recognition site and/or catalytic site. We report here the subcloning, overexpression, and a robust but novel method of production of the pure C-terminal domain of Stt3p at 60−70 mg/L in *Escherichia coli*. CD spectra indicate that the C-terminal Stt3p is highly helical and has a stable tertiary structure in SDS micelles. The well-dispersed two-dimensional $^{1}H-^{15}N$ HSQC spectrum in SDS micelles indicates that it is feasible to determine the atomic structure by NMR. The effect of the conserved D518E mutation on the conformation of the C-terminal Stt3p is particularly interesting. The replacement of a key residue, Asp^{518}, located within the WWDYG signature motif (residues 516−520), led to a distinct tertiary structure, even though both proteins have similar overall secondary structures, as demonstrated by CD, fluorescence and NMR spectroscopies. This observation strongly suggests that Asp^{518} plays a critical structural role, in addition to the previously proposed catalytic role. Moreover, the activity of the protein was confirmed by saturation transfer difference and nuclear magnetic resonance titration studies.

N-Linked glycosylation, the most ubiquitous protein modification in eukaryotic cells, is catalyzed by oligosaccharyl transferase (OT).[1] OT is a remarkably complex multisubunit enzyme that, in the case of the yeast *Saccharomyces cerevisiae*, contains nine nonidentical integral membrane protein (IMP) subunits: Ost1p, Ost2p, Ost3p, Ost4p, Ost5p, Ost6p, Stt3p, Wbp1p, and Swp1p (*1*). Among these, Ost3p and Ost6p are homologous, interchangeable subunits, while Stt3p, Wbp1p, Swp1p, Ost1p, and Ost2p are essential for the viability of the cell (*2*). In the central reaction, OT transfers a preassembled oligosaccharide moiety from a dolichol-linked pyrophosphate (Dol-PP-oligosaccharide) donor onto the side chain of the Asn of the nascent polypeptide chain specified by the N-X-T/S consensus sequence, where X can be any amino acid except proline (*1*, *3*).

N-Glycoproteins have been implicated in a multitude of cellular processes, including immune response, intracellular targeting, intercellular recognition, protein folding, and protein stability (*4*, *5*). Human genetic defects in the N-linked glycosylation pathway cause 18 inherited human disorders known as congenital disorders of glycosylation (CDG) (*6*). These conditions affect multiple organs with severe clinical manifestations, including mental retardation, developmental delay, hypoglycemia, liver dysfunction, etc. Complete loss of N-linked glycosylation is lethal to all eukaryotic organisms.

Given its extreme importance, much effort has been spent on understanding the structure and mechanisms of this enzyme complex over the past few decades. However, very limited success has been achieved with regard to the determination of structures at the atomic level. High-resolution structures of only two OT subunits have been reported. One is the NMR structure of 36-residue Ost4p, a nonessential subunit of yeast OT (*7*). The other is the crystal structure of the C-terminal domain of Stt3p from an archaea, which has very little sequence similarity to the eukaryotic Stt3p (*8*). As a result, even the most fundamental questions concerning the function of each subunit and the mechanisms of catalysis remain unanswered. The major bottleneck in research progress is due primarily to the inherent difficulties associated with the preparation of milligram quantities of IMPs, which are necessary for structure−function studies. Another barrier is finding a suitable detergent that can solubilize the protein during and after purification steps, since structure−function studies of IMPs typically rely upon detergent micelles as mimics of the native lipid bilayer. Moreover, there is no unique detergent that can solubilize every IMP and provide a stable environment for structure−function studies. Thus, finding a suitable detergent for an IMP is still very much a process of trial and error (*9*).

Stt3p is the only conserved subunit in all three domains of life (*10*). Over the past several years, an overwhelming amount of

[†]This research was financially supported by USDA PECASE (Presidential Early Career Award for Scientists and Engineers) award 2003-35302-12930, National Science Foundation Grant IBN-0628064, and National Institutes of Health Grant DK082397 (to S.M.). C.H. was supported by the ACHE-GRSP (Alabama Commission on Higher Education Graduate Research Scholars Program) Scholarship.

[‡]S.M. designed research, cloning, expression, and method development. C.H. produced proteins and collected all biophysical data. S.M. and C.H. analyzed data. S.M. and C.H. prepared the manuscript. M.B. optimized protein purification.

*To whom correspondence should be addressed: 179 Chemistry Building, Mell Street, Auburn University, Auburn, AL 36849. Telephone: (334) 844-7081. Fax: (334) 844-6959. E-mail: mohansm@auburn.edu.

[1]Abbreviations: OT, oligosaccharyl transferase; IMP, integral membrane protein; NMR, nuclear magnetic resonance; HSQC, heteronuclear single-quantum coherence; CD, circular dichroism; SDS, sodium dodecyl sulfate; DPC, dodecylphosphocholine; LDAO, lauryl dimethylamine oxide; OG, octyl β-glucoside; DDM, *n*-dodecyl β-D-maltoside; am, amidated; STD, saturation transfer difference.

Published on Web 01/04/2010

evidence indicating the direct involvement of Stt3p in the catalytic process of glycosylation in eukaryotes (*11*−*13*), the bacterium *Campylobacter jejuni* (*14*), and the archaea *Pyrococcus furiosus* (*8*) has been obtained. The most direct evidence demonstrating Stt3p as the catalytic subunit of the eukaryotic OT has come from the finding that PglB, an Stt3p homologue in *C. jejuni* bacteria, catalyzes N-linked glycosylation activity by itself. Moreover, the expression of PglB in *Escherichia coli* could enable N-linked glycosylation activity in the *E. coli* host unless point mutations were introduced into the WWDYG motif in PglB (*15*). Similarly, expression of the *Leishmania major* Stt3p homologue in yeast not only complements the yeast *STT3* deletion, it is also able to replace the entire OT complex of yeast (*16*, *17*).

Here we report the cloning, overexpression, purification, and biophysical characterization of the C-terminal domain of Stt3p. To the best of our knowledge, this is the first report of recombinant overexpression of a eukaryotic OT subunit in *E. coli*. The pure and homogeneous recombinant C-terminal domain of Stt3p was produced at a level of 60−70 mg/L of bacterial culture. In particular, we have introduced a novel, simple yet robust purification protocol involving His-tag nickel affinity chromatography without the use of any imidazole. This novel protocol has the potential to become a versatile method for the purification of other IMPs. We would like to emphasize here that the C-terminal domain of Stt3p (residues 466−718) is only soluble in detergent micelles and behaves like a membrane protein. It was previously reported that this domain is a hydrophilic lumenal domain (*10*, *18*) based on the results of topology reporter studies. However, several other TM prediction programs such as DAS (*19*), TopPred (*20*), TMpred (*21*), and SPLIT 4.0 (*22*) predict residues 564−584 to be a TM domain both for full-length Stt3p and the C-terminal domain (residues 466−718) of Stt3p. The Kyte−Doolittle algorithm predicts the presence of at least one transmembrane region (residues 564−580) located within the C-terminal domain of Stt3p. It is also very clear from our protein purification work that this domain (residues 466−718) is unusually hydrophobic in character. Whether this particular domain (residues 466−718) contains any transmembrane helices or only a few membrane-embedded residues will be clear when we determine the topology and three-dimensional (3D) solution structure.

Biophysical characterization of the C-terminal domain of Stt3p indicates that sodium dodecyl sulfate (SDS) is the most suitable detergent for structure−function studies of this protein. The C-terminal domain of Stt3p in SDS micelles is highly helical and forms a stable tertiary structure as indicated by CD studies. It is clear from the two-dimensional (2D) $^{1}H-^{15}N$ heteronuclear single-quantum coherence (HSQC) spectrum that structural characterization of the C-terminal domain of Stt3p is amenable by solution NMR.

The highly conserved WWDYG motif (residues 516−520) in the C-terminal domain of Stt3p has been reported to play a central role in the glycosylation process. Moreover, point mutations in this motif either eliminate or sharply reduce OT activity (*11*). Of particular interest is the conserved D518E mutation that results in a lethal phenotype with complete loss of N-linked glycosylation function. The extra methylene group in the glutamate side chain renders the enzyme complex completely nonfunctional (*11*). It is clear from our biophysical data that Asp^{518} plays a structural role in maintaining the conformational geometry of the active site of Stt3p for the catalysis to occur. Results of circular dichroism (CD), fluorescence, and NMR indicate that, although the D518E mutant has an overall secondary structure similar to that of the wild-type protein, its tertiary structure is remarkably different. These observations unequivocally prove that the D518E mutation does result in a dramatic conformational change in the protein, thus interfering with its function.

Furthermore, the interaction study of the C-terminal domain of Stt3p with the acceptor substrate peptide containing the N-X-T/S consensus motif was also investigated by saturation transfer difference (STD) and NMR titration experiments to confirm the biological activity of the protein.

MATERIALS AND METHODS

The detergents used in this study were sodium dodecyl sulfate (SDS) (Sigma), dodecylphosphocholine (DPC) (Anatrace), lauryl dimethylamine oxide (LDAO) (Anatrace), octyl β-glucoside (OG) (Sigma), *n*-dodecyl β-D-maltoside (DDM) (Anatrace), and digitonin (Calbiochem). For NMR studies, perdeuterated detergents were used when commercially available. The perdeuterated detergents used were SDS (Sigma, 98 at. % D) and DPC (Cambridge Isotope Laboratories, D38, >98%).

Subcloning. To clone only the C-terminal Stt3p domain protein (residues 466−718), the open reading frame (ORF) sequence was amplified using the following primers: sense, 5′-GGAATTCCATATGTCTACTTGGGTAACAAGAACTGC-3′; and antisense, 5′-CCGCTCGAGTTAGACTCTCAAGCCTAATTCAGG-3′. Yeast plasmid pRS316 containing the STT3 gene was used as the template. The fragments obtained by PCR amplification were purified, digested with *Nde*I and *Xho*I, and cloned into the *Nde*I and *Xho*I restriction sites of the pET28c vector with a His tag at the N-terminus (*Nde*I site). The orientation and sequence of the C-terminal Stt3p cDNA in the expression vector were confirmed by restriction mapping analysis and sequencing.

Mutagenesis. Oligonucleotides were specifically designed to introduce the D518E mutation. The QuickChange site-directed mutagenesis kit (Stratagene) was used to incorporate the desired mutation. The following sense and antisense primers were used (sites of mutation italicized and underlined): 5′-GTTGCAGCGTGGTGG*GAA*TACGGTTACCAAATGG-3′ (sense) and 5′-CCAATTTGGTAACCGTA*TTC*CCACCACGCTGCAAC-3′ (antisense). Incorporation of the mutation was verified by DNA sequencing.

Overexpression of Wild-Type and Mutant Proteins. The C-terminal domain (residues 466−718) of yeast Stt3p was produced in *E. coli* BL21(DE3) CodonPlus cells (Strategene) using the pET28c vector (Invitrogen). Expression of the N-terminally His_6-tagged Stt3p in the pET28c vector was under the control of an IPTG (isopropyl β-D-thiogalactopyranoside) inducible promoter. Briefly, the overnight starter culture was diluted to an OD_{600} of 0.1 in fresh LB medium containing 50 μg/mL kanamycin and grown at 37 °C to an OD_{600} of 0.4−0.6. At that point, the temperature was reduced to 30 °C and protein production was induced by the addition of IPTG to a final concentration of 0.5 mM. After 4 h, the cells were harvested by centrifugation (10000*g*) for 20 min at 4 °C and frozen at −80 °C until needed. The same protocol was followed to overexpress the D518E mutant, and the overexpression level was nearly identical to that of the wild-type C-terminal domain of Stt3p.

For the production of the ^{15}N-labeled C-terminal domain of Stt3p, cells were grown in M9 minimal medium culture containing 0.12% $^{15}NH_4Cl$ (Cambridge Isotope Laboratories). All the rest of the procedures were the same except that cells were grown for 8 h after induction with IPTG before being harvested.

Preparation of Inclusion Bodies. The *E. coli* cells containing the C-terminal domain of wild-type Stt3p (or D518E mutant) were subjected through four freeze−thaw cycles using liquid nitrogen and ice, respectively, before being resuspended in a B-PER solution (Pierce). The cells were then subjected to sonication (10×15 s); the supernatant was removed after centrifugation at 10000*g* for 30 min. The pellet was resuspended once with a 10% B-PER solution, sonicated, and centrifuged again as described above. The inclusion bodies were stored at −20 °C until needed.

Purification and Simultaneous Refolding of Wild-Type and Mutant Proteins. The inclusion bodies from the C-terminal domain of Stt3p (wild-type or D518E mutant) were dissolved in denaturing buffer containing 6 M guanidine hydrochloride (Gnd-HCl), 500 mM NaCl, and 25 mM imidazole in 20 mM phosphate buffer (pH 7.4). The insoluble materials were removed by centrifugation. The supernatant containing the solubilized C-terminal domain of Stt3p was loaded onto the Ni-NTA column (GE Healthcare) which was pre-equilibrated with binding buffer [500 mM NaCl, 25 mM imidazole, and 20 mM phosphate buffer (pH 7.4)]. Impurities were removed using a washing buffer [20 mM phosphate buffer (pH 7.4), 500 mM NaCl, 200 mM imidazole, and 1% Triton X-100 (v/v)] several times with shaking. To remove imidazole and NaCl from the protein sample before elution, a final wash was followed with 20 mM phosphate buffer (pH 6.5). The absorbance of the washing was monitored by measuring the OD_{280} until there was no apparent reading. We conducted elution and simultaneous refolding by loading elution buffer [50 mM SDS, 1% glycerol, and 20 mM phosphate buffer (pH 6.5)] onto the column followed by shaking for at least 2 h. To keep the protein concentration high, the volume of elution buffer added was kept to a minimum (< 1 mL). The elution was continued until there was no more absorbance as monitored by OD_{280} readings. The protein concentration was calculated from the A_{280} using an extinction coefficient of 63083 M^{-1} cm^{-1} (*23*). The purity of the protein in each elution was assessed by SDS−PAGE analysis. The pure protein samples were kept at room temperature away from light.

Matrix-Assisted Laser Desorption Ionization (MALDI) Time-of-Flight Mass Spectrometry. The protein sample for MALDI-TOF measurement was prepared in 10 mM SDS and 20 mM ammonium acetate buffer. The target was spotted as follows. The protein sample was mixed with the matrix [10 mg/mL sinapinic acid (SA) in a 4:6 methanol/water mixture, with 0.1% trifluoroacetic acid] in a 1:4 ratio for a total of 1 μL. The entire solution was applied to target and allowed to air-dry. MALDI mass spectra were recorded on an Autoflex II TOF mass spectrometer from Bruker. The spectra were acquired in linear mode using the following settings: laser power, 55%; ion source 1, 20 kV; ion source 2, 18 kV; lens, 6.50 kV; number of shots, 50; detection, from 10000 to 100000.

NMR Sample Preparation. Each sample for NMR measurement was concentrated to 0.2 mM using an Amicon Ultra-15 (molecular mass cutoff of 5 kDa) centrifugal ultrafiltration cartridge. The final NMR sample was in 20 mM phosphate buffer (pH 6.5), 1 mM EDTA, 100 mM SDS, and 10% D_2O (v/v). In this study, besides SDS, five other detergents were screened to determine the most suitable membrane mimetic for the C-terminal Stt3p domain. These detergents are DPC, LDAO, OG, DDM, and digitonin. The protein samples in these detergents were prepared by buffer exchange of the protein in SDS detergent with the desired detergent by using an Amicon ultrafiltration device with a molecular mass cutoff of 5 kDa. Typically, 500 μL of the desired detergent solution was added to 500 μL of SDS-containing protein sample in an Amicon Ultra-15 tube and centrifuged until there was approximately 500 μL of solution left. This process was repeated 10 times for complete detergent exchange.

NMR Measurement. $^1H-^{15}N$ HSQC spectra were recorded for both the wild type and D518E mutant of the C-terminal domain of Stt3p. NMR measurements were taken at 308 K. Data were collected on a Bruker Avance 600 MHz spectrometer fitted with a cryogenic triple-resonance probe equipped with *z*-axis pulsed field gradients. The data were acquired with 256 and 2048 complex points in the t_1 time domain (^{15}N dimension) and t_2 time domain (^1H dimension) respectively. The data were zero-filled to 512×4096 and apodized using a Gaussian window function prior to Fourier transformation using NMRPipe (*24*).

Circular Dichrosim (CD) Spectropolarimetry. All CD experiments were performed on a JASCO J-810 automatic recording spectropolarimeter using a 0.05 cm path length quartz cell at room temperature. The wild-type C-terminal domain of Stt3p was assessed in both SDS and DPC micelles, while D518E was assessed only in SDS micelles. The buffer used was 20 mM phosphate buffer (pH 6.5). The protein concentration was 10 μM for far-UV CD measurement and 89 μM for near-UV CD measurement. Data were averaged over 100 scans with a response time of 1 s and a scan speed of 100 nm/min. CD data were converted to mean residual ellipticity (θ) by standard procedures.

Fluorescence. All fluorescence spectra were recorded on a Perkin-Elmer Precisely LS 55 luminescence spectrofluorometer. All experiments were conducted in 10 mM phosphate buffer (pH 6.5) containing 1 μM protein at 25 °C. The data were recorded by monitoring intrinsic tryptophan fluorescence (excitation at 280 nm and emission at 300−500 nm).

Ligand Binding Studies by Saturation Transfer Difference (STD) NMR Spectroscopy. For STD studies, the methyl-protonated {Ile(δ_1 only), Leu($^{13}CH_3$,$^{12}CD_3$), Val($^{13}CH_3$, $^{12}CD_3$)} U-{^{15}N,^{13}C,^2H} labeled C-terminal domain of Stt3p was overexpressed by using the same cell line and vector as described above. Briefly, the transformed cells picked from the LB agar plate were grown in 3 mL of LB medium at 37 °C for 3 h, then transferred to 25 mL of unlabeled M9/H_2O minimal medium, and grown until the OD_{600} reached ∼0.5. The cells were then separated from the medium by centrifugation at 3000 rpm for 15 min and transferred to 100 mL of M9/D_2O culture containing 0.12% (m/v) $^{15}NH_4Cl$ as the sole nitrogen source and 0.4% (m/v) [^{13}C,^2H]glucose (Cambridge Isotope Laboratory, Andover, MA) as the sole carbon source. At an OD_{600} of ∼0.5, the culture was diluted to 500 mL with M9/D_2O medium. One hour prior to induction, 35 mg of 2-keto-3,3-d_2-[1,2,3,4-^{13}C]butyrate (Sigma Aldrich) and 60 mg of 2-keto-3-methyl-d_3-3-d_1-[1,2,3,4-^{13}C]butyrate (Sigma Aldrich) were added to the medium. The expression of the protein was induced at an OD_{600} of ∼0.4 with 0.5 mM IPTG, and the culture was allowed to grow for an additional 11−12 h at 30 °C (final OD_{600} of ∼2.0), at which point the cells were harvested by centrifugation. The protocols for cell lysis and purification were the same as those described previously.

The six-residue peptide (Tyr-Asn-Ser-Thr-Ser-Cys-Am, purity of >99%) was custom synthesized by Biomatik USA, LLC. The protein NMR sample for the STD experiment was prepared in 20 mM phosphate buffer (pH 6.5), containing 100 mM perdeuterated SDS and 10% D_2O. Protein and substrate peptide

concentrations in the NMR sample were 30 and 300 μM, respectively.

The STD measurements were performed on a Bruker Avance 600 MHz spectrometer fitted with a cryogenic triple-resonance probe equipped with *z*-axis pulsed field gradients at 308 K. The irradiation power was set to $(\gamma/2\pi)B_1$ = 20 Hz, which was applied on-resonance at 0.738 ppm, where no peptide signals were present, or off-resonance at 100 ppm, where no protein signals were present. To efficiently saturate the entire protein by spin diffusion, we set the saturation time to 10 s. A 50 ms spin-lock pulse ($T_{1\rho}$ filter) was used to eliminate the background protein resonances to facilitate analysis. The spectra were recorded in an interleaved pseudo-2D fashion to reduce temporal fluctuations. AU program "stdsplit" from TOPSPIN version 2.1 (Bruker) was used to subtract the unprocessed on- and off-resonance spectra.

Ligand Binding Studies by NMR HSQC Titrations. To measure dissociation constants (K_D), we collected a series of 2D $^1H-^{15}N$ HSQC spectra with progressive additions of substrate peptide (Asn-Asp-Thr-NH_2) to ^{15}N-labeled C-terminal Stt3p to attain protein to peptide molar ratios of 1:0, 1:0.5, 1:1, 1:5, 1:10, 1:20, 1:35, 1:50, 1:75, and 1:100. The starting sample contained 170 μM protein in 20 mM phosphate buffer (pH 6.5), 100 mM SDS, 5% D_2O, 1% glycerol, and 5 mM Mg^{2+}. The peptide with > 95% purity was custom synthesized by Genemed Synthesis, Inc. (South San Francisco, CA). NMR data collection and processing were the same as previously described. The chemical shift changes of the affected residues of the protein were plotted against the peptide concentration and fitted by Hill model in Origin version 7.0 (Microcal). Chemical shift perturbations were calculated as $[(\delta^1H)^2 + (\delta^{15}N/5)^2]^{1/2}$, in which δ^1H and $\delta^{15}N$ are changes in chemical shift for ^1H and ^{15}N, respectively.

RESULTS

Overexpression and Purification of Wild-Type and Mutant Proteins. It is imperative to produce milligram quantities of pure protein for structural characterization of any protein. This requirement and the necessity of a suitable membrane mimetic are formidable obstacles to structural characterization of IMPs. To date, there are no reports of recombinant expression of any eukaryotic OT subunit in *E. coli* or in any other heterologous system. This deficiency seriously impedes any biophysical and/or biochemical research on N-linked glycosylation. After many trials, we were able to overexpress the C-terminal domain of Stt3p with an N-terminal His_6 tag in the pET-28c vector using *E. coli* strain BL21(DE3) CodonPlus (Figure 1). Protein expression was optimized using different *E. coli* strains, temperatures, and IPTG concentrations (see Materials and Methods for details). The target protein was expressed in inclusion bodies, which is quite common for eukaryotic membrane proteins since these proteins are often not well incorporated into the plasma membrane of *E. coli*.

Inclusion bodies were solubilized by using 6 M Gdn-HCl, followed by binding to Ni(II) metal ion affinity resin, and all of the impurities were washed off. Detergent was used during purification processes since the C-terminal Stt3p domain was found to be a water insoluble protein. The standard protocol is the use of imidazole to compete off the His-tagged protein from the Ni-NTA resin. However, this simple procedure did not work well for the C-terminal Stt3p domain. Most of the protein remained bound to the Ni-NTA resin even when the imidazole concentration was increased to ~2 M in the elution buffer

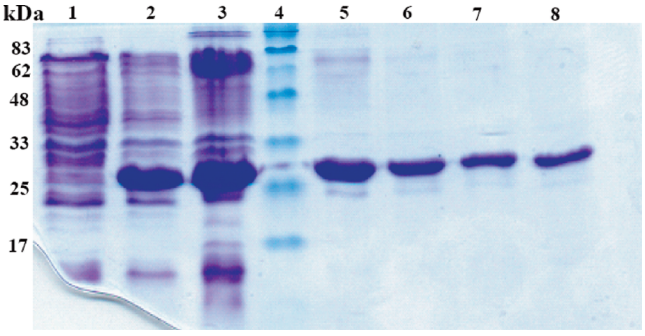

FIGURE 1: Coomassie-stained SDS−PAGE of samples from a typical C-terminal Stt3p expression and purification run. The mobility of the His-tagged C-terminal Stt3p in the SDS−PAGE gel is compatible with its molecular mass (31.4 kDa): lane 1, before induction; lane 2, 4 h after induction with 0.5 mM IPTG; lane 3, inclusion body; lane 4, protein molecular mass markers; lanes 5−8, protein purified by "SDS Elution" where elution fractions 1−4, respectively, are shown.

containing digitonin (as analyzed by SDS−PAGE). It was clear that there are other interactions, most likely between the hydrophobic regions of the protein and the resin, that play a major role in the binding. This observation was proven to be correct when the His-tagged C-terminal domain was able to efficiently bind even to EDTA-treated Ni^{2+}-depleted resin. Thus, developing a method for the elution of the protein off of the resin was unavoidable.

Here, we report a novel, simple yet robust purification protocol for purifying the C-terminal Stt3p domain without using imidazole. The protein bound to the Ni-NTA resin was efficiently eluted off of the column with buffer containing 50 mM SDS in 20 mM phosphate buffer (pH 6.5) after the column had been shaken for 2 h at room temperature. Indeed, the first several elutions (500 μL of each eluted fraction) contained ~200 μM pure protein (Figure 1). However, the C-terminal Stt3p domain could also be eluted off of the Ni-NTA column with SDS concentration as low as 10 mM. In fact, this method also worked for the elution of the protein from Ni^{2+}-depleted resin. SDS was then freely exchanged with any other detergent by following the protocol described in Materials and Methods.

The D518E mutant was expressed and purified following the same protocol that was used for the wild-type protein. The level of overexpression and the yield of pure protein obtained for the mutant were comparable to those of the wild-type protein.

Determination of Mass by MALDI-TOF Mass Spectrometry. Relative mobilities of polypeptide chains in SDS−PAGE can be used to assign tentative molecular masses; however, this is purely an empirical procedure. Thus, MALDI-TOF mass spectrometry was utilized to confirm the mass of the purified protein. However, this simple approach was complicated by the presence of SDS. Several reports have demonstrated that SDS is detrimental to MALDI-MS (*25*−*27*). After numerous optimizations, eventually, the appropriate conditions, including solvent system, matrix type, and concentration of SDS, were determined for the collection of reliable MALDI signals. Ammonium acetate buffer was found to be essential, and the SDS concentration was optimal at 10 mM. The mass spectrum of the purified protein exhibited a molecular ion at *m*/*z* 31493.1 (Figure 2). This is in accordance with the calculated mass of 31502.3 Da for the His-tagged C-terminal domain of Stt3p as calculated by the ProtParam tool of expert protein analysis system (ExPASy) (*28*). With MALDI-TOF data, a margin of error of 0.15% is acceptable (*29*); however, for our data, the margin of error was only 0.03%.

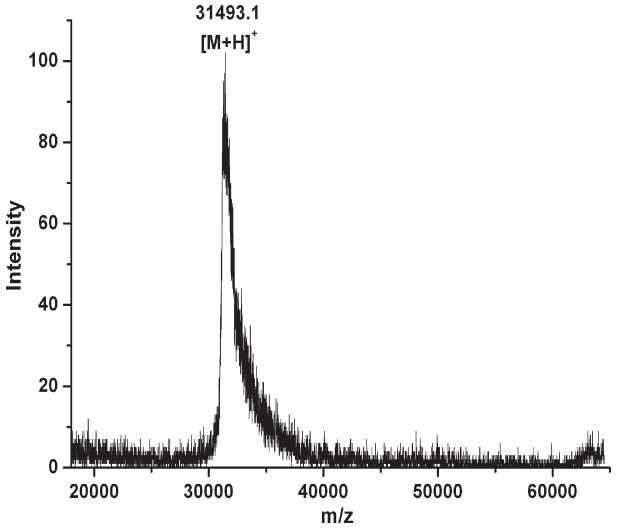

FIGURE 2: MALDI-TOF analysis of the molecular mass of the purified His-tagged C-terminal domain of Stt3p. The mass spectrum of the purified protein exhibited a molecular ion at m/z 31493.1, which is in accordance with the calculated value (31502.3 Da) for the His-tagged C-terminal domain of Stt3p.

Detergent Screening by NMR Spectroscopy. Since it is not currently possible to determine the best detergent a priori, in this study, a number of different detergents, including SDS, DPC, LDAO, OG, digitonin, and DDM, were screened. During the detergent exchange process with LDAO, the protein precipitated, indicating that LDAO is not an appropriate detergent for solubilizing the C-terminal domain of Stt3p. The five detergents were screened by NMR spectroscopy to determine their suitability for reconstitution of the C-terminal domain of Stt3p. The 2D HSQC spectrum provides both qualitative and quantitative information for the evaluation of whether a protein is well-folded and exists in a single conformation. The quality and number of peaks present in a 2D HSQC NMR spectrum reveal whether a protein is monomeric or if it exists in oligomeric forms. This information is vital for assessing the feasibility of further solution NMR-based structural characterizations. As shown in Figures 3 and 4, the quality of HSQC spectra varies markedly as a function of detergent. The HSQC spectrum of the C-terminal domain of Stt3p in DPC micelles, a detergent often found to provide high-quality NMR spectra for membrane proteins (*30*), showed very broad line widths and a number of missing resonances. Digitonin and DDM micelles produced poorly resolved spectra (Figure 3). These observations clearly demonstrate that the C-terminal domain of Stt3p is oligomerized in the micellar environments described above. Oligomerization leads to slower tumbling and rapid transverse relaxation rates, which substantially broaden and weaken the resonances, thus dramatically reducing spectral resolution. In the case of the detergent OG, more peaks than expected were observed in the HSQC spectrum, indicating the presence of multiple conformations or oligomeric equilibria. Of the five detergents tested, SDS was determined to be the best for further NMR-based structural characterization. It produced a far superior spectrum (Figure 4) with favorable dispersion and narrow line widths, indicating that the C-terminal domain of Stt3p was folded into a single stable conformation under the experimental condition. Furthermore, of 263 non-proline residues, 245 resolved peaks with relatively uniform intensity were counted.

The optimal concentration of SDS was determined by thoroughly investigating the effect of SDS on protein conformation by

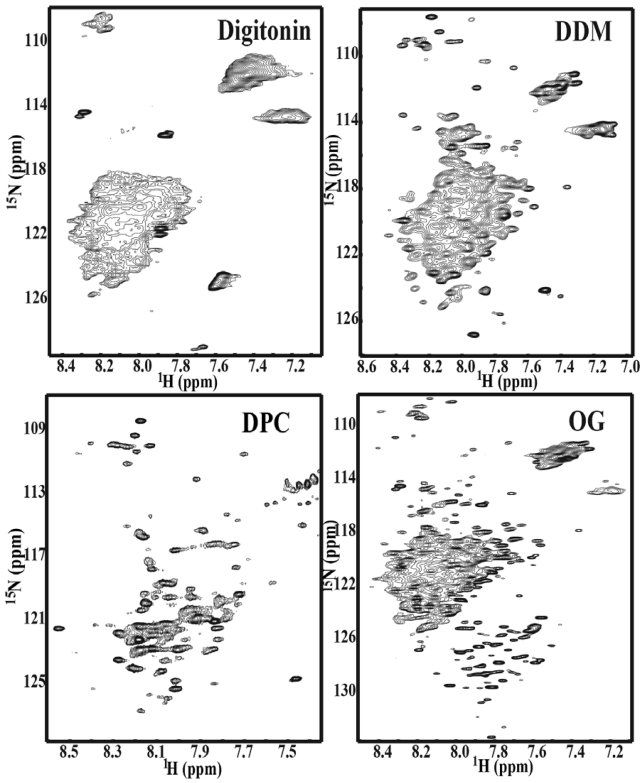

FIGURE 3: 2D NMR $^1H-^{15}N$ HSQC spectra of the purified [U-^{15}N]-His-tagged C-terminal domain of Stt3p at a concentration of ~0.2 mM in 20 mM phosphate buffer containing 5% D_2O (pH 6.5) in different detergent micelles. The concentrations of detergents were as follows: 1.5% digitonin, 1% DDM, 300 mM DPC, and 150 mM OG.

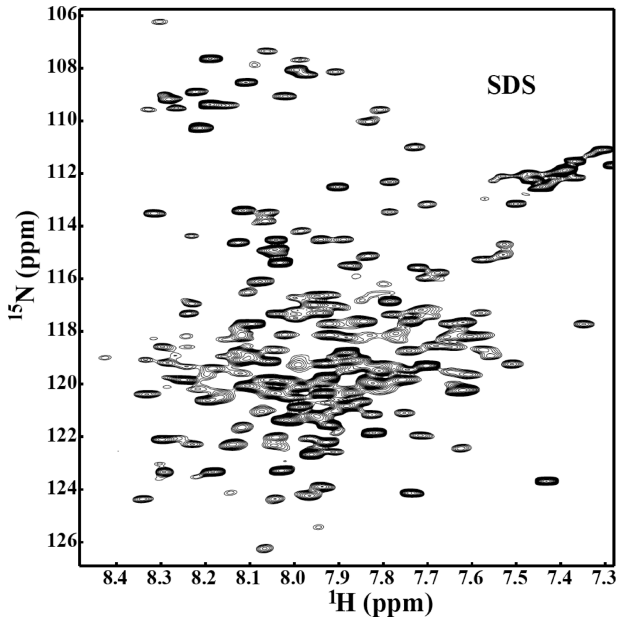

FIGURE 4: 2D NMR $^1H-^{15}N$ HSQC spectrum of the purified [U-^{15}N]-His-tagged C-terminal domain of Stt3p at a concentration of ~0.2 mM in 20 mM phosphate buffer containing 5% D_2O (pH 6.5) with 100 mM SDS.

NMR. Our data indicated that the HSQC spectra were well resolved and closely resembled one another when the SDS concentration was in the range of 50−200 mM (Figure 5A−C). However, the spectra started to lose their resolution at concentrations above 250 mM. When the SDS concentration was increased to

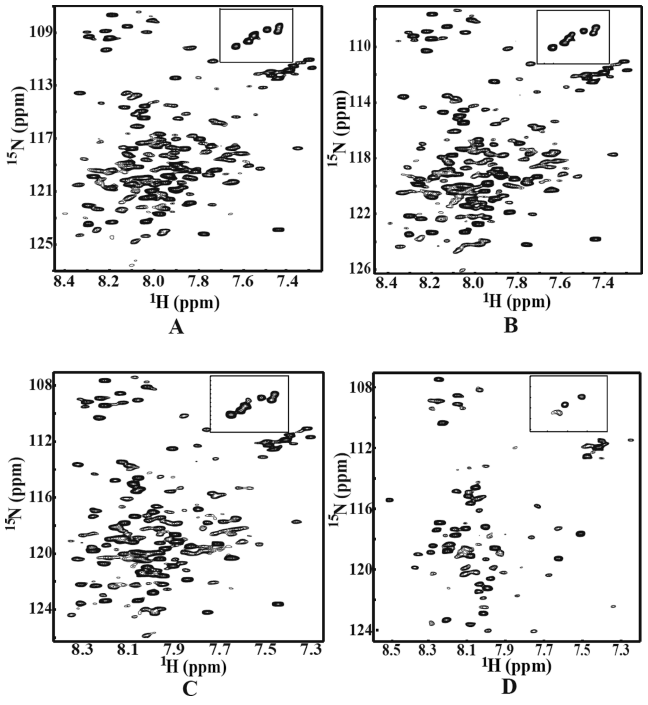

FIGURE 5: 2D NMR ^{1}H−^{15}N HSQC spectra of the purified [U-^{15}N]-His-tagged C-terminal domain of Stt3p [in 20 mM phosphate buffer and 5% D_2O (pH 6.5)] as a function of SDS concentration. Each inset is a close-up view of the tryptophan indole amide proton region from the same spectrum. The concentrations of SDS were as follows: (A) 50, (B) 100, (C) 200, and (D) 400 mM.

≥400 mM, the resonance dispersion became very narrow with many missing peaks, indicating that the protein had partially denatured (Figure 5D). Altogether, 100 mM SDS was chosen as the working condition for further characterization.

Characterization of the C-Terminal Domain of Stt3p by Far-UV and Near-UV CD Spectroscopy. Far-UV and near-UV CD spectroscopy were employed to probe the secondary and tertiary structure of the C-terminal domain of Stt3p in 100 mM SDS micelles and 400 mM DPC micelles for the sake of comparison. The far-UV CD spectra (Figure 6A) in both SDS and DPC micelles had the characteristics of a typical α-helical protein with CD minima at 208 and 222 nm. This observation is consistent with what was seen in the 2D HSQC spectrum, namely, relatively narrow proton dispersion, which is another indication of a helical protein. These results are also consistent with the crystal structure of its recently reported archaea homologue (*8*), even though there are only limited sequence similarities between these two proteins.

Near-UV (250−350 nm) CD spectra are due to the dipole absorption of the aromatic residues and disulfide bonds (if present), which depends upon the orientation and nature of the surrounding environment of these chromophores and is therefore sensitive to the overall tertiary structure of a protein (*31*−*33*). For a protein in an unfolded or molten globule state, one of the classical spectroscopic signatures is the absence of a near-UV signal (*34*). In other words, the presence of significant near-UV signals is a strong indication that the protein is folded into a well-defined structure. The presence of a near-UV CD signal for the C-terminal domain of Stt3p in 100 mM SDS (Figure 6B) indicates that the protein has a well-defined tertiary structure. Interestingly, the tertiary structure appears to be disrupted in DPC micelles (Figure 6B), which is consistent with the NMR data (Figure 3C) despite the widely accepted notion

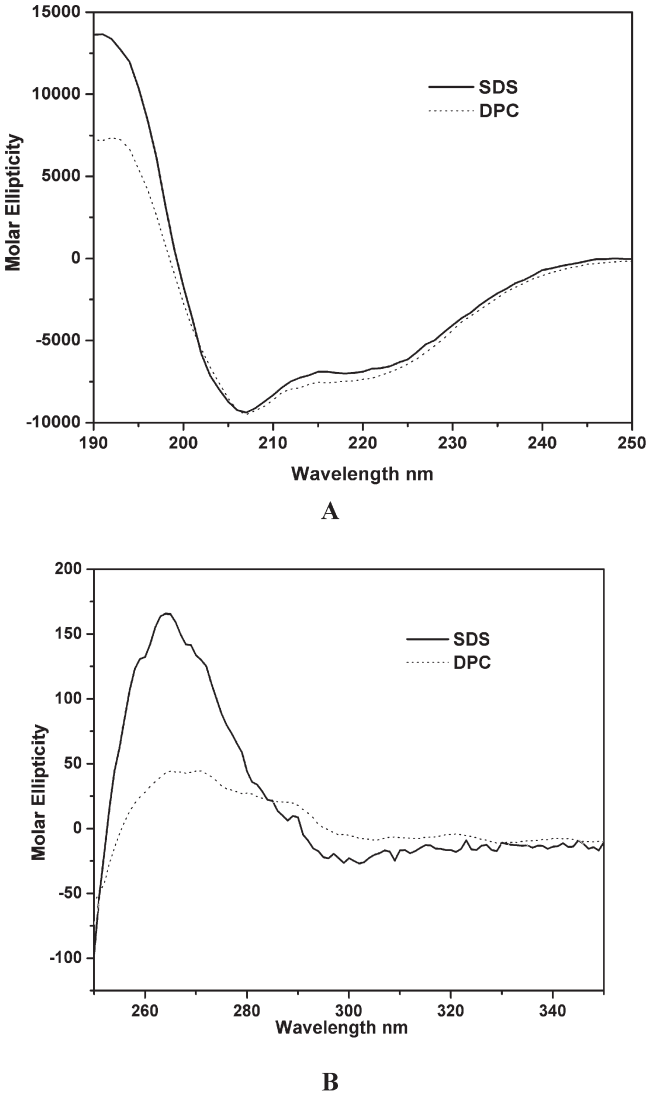

FIGURE 6: Circular dichroism (CD) spectroscopic analysis of the C-terminal domain of Stt3p at room temperature. (A) Far-UV CD spectra of the C-terminal domain of Stt3p in 300 mM DPC and 100 mM SDS detergent micelles. The protein concentration was 10 μM in 20 mM phosphate buffer (pH 6.5). The characteristic double minima at 208 and 222 nm are indicative of significant α-helical content. (B) Near-UV CD spectra of the C-terminal domain of Stt3p in 300 mM DPC and 100 mM SDS detergent micelles. The protein concentration was 89 μM, and the buffer conditions were the same as those described for panel A.

that DPC is usually a "milder" detergent that generally does not denature proteins. Close inspection of the near-UV CD spectrum in SDS micelles reveals that there are three humps, from left to right, which can be attributed to the absorption of phenylalanine, tyrosine, and tryptophan, respectively.

Intrinsic Tryptophan Fluorescence. Intrinsic fluorescence, especially with tryptophan as a probe, provides a powerful analytical tool for membrane protein studies because of its sensitivity and simplicity (*35*). The fluorescence emission spectrum of the C-terminal domain of Stt3p (containing eight tryptophan residues) upon excitation at 280 nm exhibited a broad emission spectrum with λ_{max} ranging from 330 to 350 nm (Figure 7C). This result indicates that of the eight tryptophan residues, some are totally buried in the hydrophobic core, some are partially exposed to water, and the rest are completely exposed to water. This result is not surprising since in integral membrane

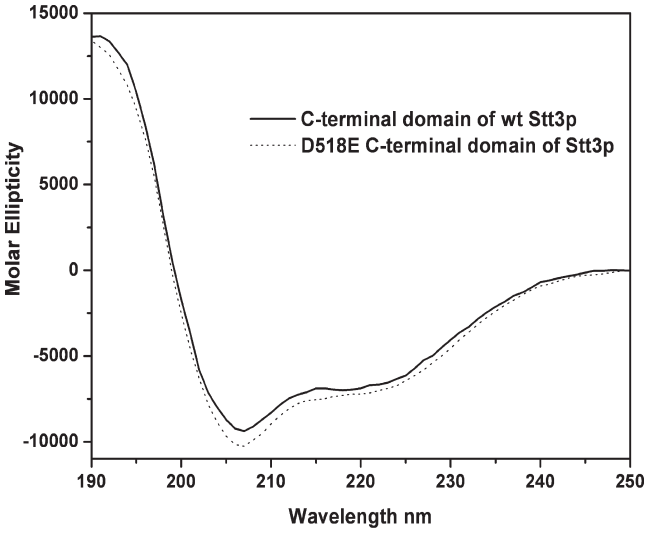

A

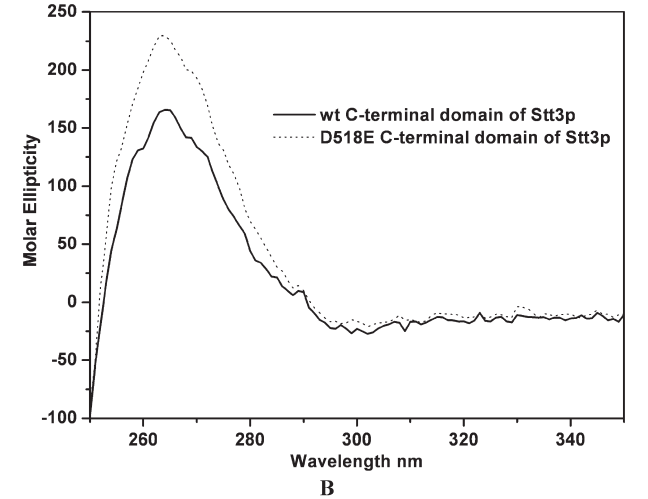

B

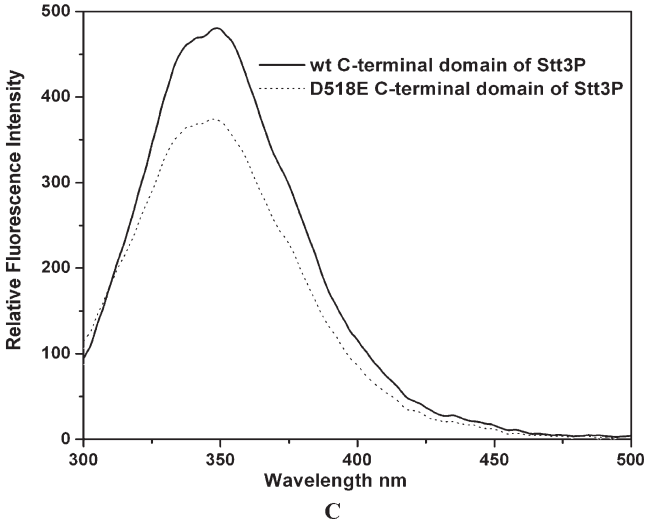

C

FIGURE 7: CD and fluorescence spectra of the wild type and D518E mutant of the C-terminal domain of Stt3p. The data were collected under the same conditions. (A) Far-UV CD spectra. The protein concentrations were 10 μM in 20 mM phosphate buffer (pH 6.5) and 100 mM SDS. (B) Near-UV CD spectra. The protein concentrations were 89 μM in 20 mM phosphate buffer (pH 6.5) and 100 mM SDS. (C) Intrinsic tryptophan fluorescence spectra. The protein concentrations were 1 μM in 10 mM phosphate buffer (pH 6.5) and 100 mM SDS. The introduction of the mutation leads to an intensity quench and blue shift of the spectrum.

proteins, tryptophan residues have been found to show preferential clustering at the membrane interface (*36*−*41*). The exact location and orientation of each tryptophan residue can only be clear once the high-resolution 3D structure of the C-terminal domain of Stt3p is determined.

Comparison of Wild-Type and Mutant Proteins. In the C-terminal domain of Stt3p, residues 516−520, which make up the WWDYG motif, are highly conserved through several branches of the evolutionary tree. This motif is thought to be directly involved in the glycosylation site recognition and/or in the catalytic glycosylation process on the basis of co-immunoprecipitation, photoaffinity labeling, and both block- and single-mutation analysis (*11*). Furthermore, subtle substitution of a single residue such as Asp^{518} with Glu renders the enzyme completely inactive, causing cell death in the yeast *S. cerevisiae* (*11*). This observation demonstrates that there may be a strict geometric or conformational requirement for the enzyme to catalyze the N-linked glycosylation reaction. To investigate whether Asp^{518} acts only as a catalytic base as proposed previously (*11*) or has any role in the conformational geometry required for catalysis, we conducted biophysical characterization of both the wild type and the D518E mutant under identical conditions. The far-UV CD spectra (Figure 7A) of the wild-type Stt3p C-terminal domain and the D518E mutant are very similar, suggesting that there is no significant change in the secondary structure with this point mutation. In contrast, there are significant differences in the near-UV CD spectra, which reveal that both of the proteins have distinct tertiary structures (Figure 7B). This evidence is further supported by measurements of their tryptophan fluorescence spectra. The D518E mutation led to an apparent blue shift as well as quenching of the actual intensity of the fluorescence emission of the wild-type protein (Figure 7C), indicating the change in the microenvironments of the tryptophan residues. This observation demonstrates that the D518E mutation indeed changes the structure of the C-terminal domain of Stt3p, affecting the microenvironment and solvent exposure of some tryptophan residues, most likely neighboring W516 and W517 (*36*, *42*).

NMR is an extremely robust technique for monitoring the changes in the conformation of a protein sample due to changes in pH, temperature, salt, or addition of a ligand. The 2D $^{1}H-^{15}N$ HSQC spectrum represents the fingerprint region of a protein. This region is extremely sensitive, and any perturbation in the chemical shifts or resonances from the original positions is an indication of a change in the conformation of the protein. This change can be local, involving few residues or a global conformational change involving most of the residues in the protein. In this study, HSQC spectra were collected to compare the fingerprint region of the wild type and the D518E mutant in SDS micelles under identical conditions. It is clear from Figure 8 that the D518E point mutation induced drastic changes in the chemical shift positions of a number of peaks, indicating that the wild type and the D518E mutant have distinctly different conformations. This conformational change cannot be attributed simply to a change in the local environment around Asp^{518} since the chemical shift perturbation is dramatic for most of the peaks in the HSQC spectrum. In fact, some of the resonances observed in the wild-type HSQC spectrum disappeared in the spectrum of the mutated protein. This observation demonstrates that the D518E mutation indeed affects both the conformation and dynamics of the wild-type protein, which may have a bearing on OT function.

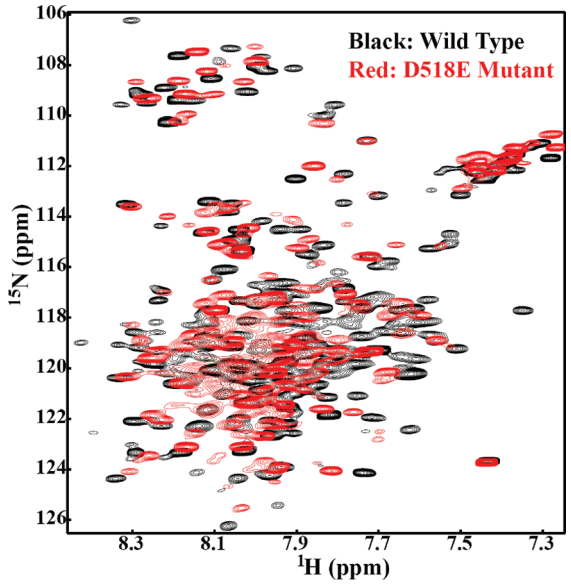

FIGURE 8: Impact of the D518E mutation on the 2D ^{1}H−^{15}N HSQC spectrum. The black spectrum represents that of the wild type, while the superimposed red spectrum is that of the D518E mutant of the C-terminal domain of Stt3p.

Acceptor Substrate Binding Studies by STD NMR Spectroscopy. To investigate the interactions of the acceptor substrate of OT with the C-terminal domain of Stt3p, binding studies were conducted with a six-residue peptide containing the consensus N-linked glycosylation sequon by saturation transfer difference (STD) NMR spectroscopy. STD has been proven to be a powerful method for probing low-affinity interactions ($K_D \approx 10^{-8}$ to 10^{-3} M) of small molecules with proteins (*43*−*48*). In the STD technique, selective saturation of a protein resonance leads to a rapid spread of the magnetization over the entire protein *via* spin diffusion, and intermolecular transfer of magnetization from the protein to ligand leads to changes in the NMR signal intensity of the ligand. However, for interaction studies involving proteins and peptides, attention should be paid to make sure a well-separated peak in the protein is picked for the STD experiment. Thus, the saturation resonance must exclusively belong to the protein. Moreover, the resulting signals in STD spectra must exclusively belong to the peptide ligand. The latter is especially true if incomplete protein signal suppression occurs.

To overcome these, here, a methyl-protonated {Ile(δ_1 only), Leu($^{13}CH_3$,$^{12}CD_3$), Val($^{13}CH_3$,$^{12}CD_3$)} U-{^{15}N,^{13}C,^{2}H} labeled sample (ILV-sample) of the C-terminal domain of Stt3p was prepared by using biosynthetic precursors (*49*) . This labeling pattern is extremely desirable for STD studies since in these labeled proteins, except for water-exchangeable protons, only the methyl groups of the Ile (δ_1 only), Leu, and Val residues are protonated. In the ILV-sample, the commonly used regions for irradiation of the protein remain, such as the upfield region (~0 ppm) or downfield region (~10 ppm). Additionally, the simplified protein spectrum facilitates the data analysis process significantly and reduces the risk of having the pseudopositive effect that resulted from incomplete elimination of background protein signals. As shown in Figure 9, the C-terminal domain of Stt3p and peptide ligand complex was irradiated at 0.738 ppm, where no peptide NMR signal was present. Peaks a−f in the STD spectrum exclusively correspond to peaks 1−6, respectively, in the NMR spectrum of the acceptor peptide (Figure 9B,C). The appearance of the NMR peaks of the peptide ligand in the

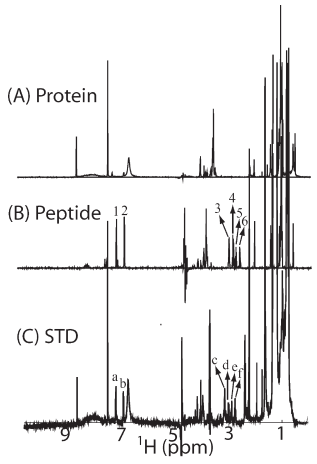

FIGURE 9: (A) One-dimensional (1D) NMR spectrum of the methyl-protonated {Ile(δ_1 only), Leu($^{13}CH_3$,$^{12}CD_3$), Val($^{13}CH_3$,$^{12}CD_3$)} U-{^{15}N,^{13}C,^{2}H} labeled sample of the C-terminal domain of Stt3p (30 μM) in 20 mM phosphate buffer (pH 6.5) and 100 mM deuterated SDS. (B) 1D NMR spectrum of 300 μM peptide ligand, Tyr-Asn-Ser-Thr-Ser-Cys-Am, in 20 mM phosphate buffer (pH 6.5) and 100 mM deuterated SDS. (C) STD NMR spectrum of the complex of the methyl-protonated {Ile (δ_1 only), Leu($^{13}CH_3$,$^{12}CD_3$), Val($^{13}CH_3$,$^{12}CD_3$)} U-{^{15}N,^{13}C,^{2}H} labeled sample of the C-terminal domain of Stt3p and acceptor peptide substrate (Tyr-Asn-Ser-Thr-Ser-Cys-Am) in 20 mM phosphate buffer (pH 6.5) and 100 mM deuterated SDS. The protein and peptide concentrations are 30 and 300 μM, respectively. The spectrum was recorded with a $T_{1\rho}$ filter, consisting of a 50 ms spin-lock pulse, to eliminate the resonances of the protein. The appearance of peaks a−f in the STD spectrum, which correspond to peaks 1−6, respectively, in the NMR spectrum of acceptor peptide, reveals the C-terminal domain of Stt3p binds to the acceptor substrate of OT.

difference spectrum unequivocally indicates that the acceptor peptide ligand is bound to the C-terminal domain of Stt3p. More importantly, close inspection of the difference spectrum reveals that the amide protons (peak a, which has a chemical shift of 7.13 ppm) on the side chain of the Asn residue, the N-glycosylaiton site, are significantly affected by the saturation pulse (Figure 9C), which strongly suggest that the side chain of the Asn residue is directly involved in the protein−substrate recognition process.

Affinity Studies by NMR Titrations. To further determine the affinity of the acceptor substrate (of OT) with the recombinant C-terminal domain of Stt3p, titration studies were conducted with the Asn-Asp-Thr-NH_2 acceptor peptide containing the consensus N-linked glycosylation sequon. Substrate binding was followed by monitoring the changes in chemical shift positions in the fingerprint region of the protein in 2D HSQC spectra as shown in Figure 10A. The chemical shift perturbations of four representative peaks were fitted to a Hill model by using Origin version 7.0, and the plot is shown in Figure 10B. It is clear from the fit that the C-terminal domain of Stt3p exhibits a sigmoidal saturation curve and binds to the acceptor peptide with an apparent K_D of 9.97 ± 0.44 mM. The Hill coefficient "*n*" is 1.70, suggesting positive cooperativity (as $n > 1$) in binding with a relatively low affinity.

DISCUSSION

High-Level Protein Expression and Purification. Although N-linked glycosylaiton is an essential, critical, and highly conserved process in all eukaryotes, very little structural and functional information about the OT enzyme complex is known, the primary reason being the difficulties in the production of milligram

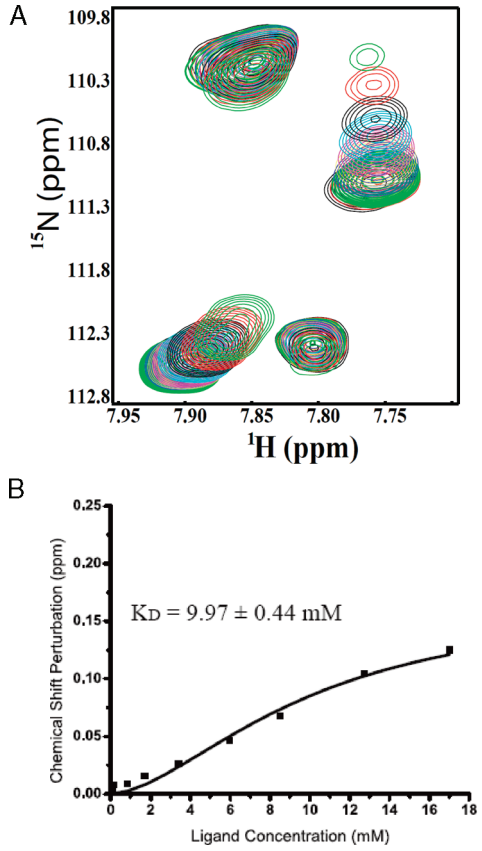

FIGURE 10: (A) Expanded region of the overlay of 2D ^{1}H−^{15}N HSQC spectra of the [U-^{15}N] labeled C-terminal domain of Stt3p (170 μM) showing changes in the chemical shift positions upon addition of increasing concentrations of the substrate peptide. Ratios of protein to peptide were 1:0 (black), 1:0.5 (red), 1:1 (green), 1:5 (blue), 1:10 (yellow), 1:20 (purple), 1:35 (cyan), 1:50 (black), 1:75 (red), and 1:100 (green). (B) Chemical shift perturbation average of four representative resonances plotted as a function of the concentration of the substrate peptide and fitted using the Hill model of Origin version 7.0.

quantities of integral membrane proteins (IMPs) for structural or functional characterization. Recombinant expression of IMPs in *E. coli*, the primary machine for large-scale protein production for structural studies, has had very limited success (*50*). As a result, there is only one example of recombinant expression of an OT subunit from prokaryotic sources, which is the water-soluble C-terminal domain of the Stt3p homologue from the archaea *P. furiosus* (*51*).

Here we report a high-level recombinant expression in *E. coli* and purification of the C-terminal domain of Stt3p from the yeast *S. cerevisiae*. This is the first report of heterologous expression of a eukaryotic OT subunit. This high-level production of the pure C-terminal domain of Stt3p makes isotopic labeling for structural characterization by either solution NMR or X-ray crystallography straightforward, affordable, and, most importantly, possible.

After many unsuccessful attempts to refold the denatured C-terminal domain of Stt3p in aqueous solution without the use of any detergents, we were convinced that a membrane mimetic environment is necessary for both its purification and reconstitution. This evidence suggests that the C-terminal domain of Stt3p may contain at least one TM helix or several membrane-embedded residues. Purification and reconstitution of membrane proteins are notoriously difficult tasks. Indeed, reports of successful isolation and refolding of IMPs from inclusion bodies have thus far been limited to a small number of proteins (*52*−*54*). In an elegant work, Page and co-workers reported two methods for isolation and purification of helical integral membrane proteins: "detergent exchange" and "reconstitution". Both of these methods use standard protocols for detergent-mediated purification *via* Ni^{2+} affinity chromatography (*30*). Here, we report a novel method for the one-step purification and reconstitution of the C-terminal domain of Stt3p that we have named "SDS elution". Using our novel method, we were able to obtain a very high yield of purified protein (60−70 mg of protein per liter of bacterial culture) in a single step. To evaluate the efficiency of our method, we also produced ^{15}N-labeled C-terminal Stt3p following the reconstitution method of Page et al. (*30*). After the precipitated proteins were reconstituted in 100 mM SDS and 300 mM DPC micelles as per the reconstitution method (*30*), the HSQC spectra were recorded and compared with the spectra of the samples prepared by our SDS elution method. Although the HSQC spectra were similar overall (data not shown), the spectra for the protein obtained by the reconstitution method appeared to be deteriorated, possibly because of aggregation. Moreover, the protein yield obtained by the SDS elution method was much higher. Indeed, in principle, SDS elution combines both detergent exchange and reconstitution but greatly simplifies these protocols.

This novel methodology has several advantages over the conventional methods. First and foremost, with our method, purification and reconstitution are achieved simultaneously, which dramatically shortens the sample preparation process. Second, since there is no imidazole in elution buffer, the conventional method of removal of imidazole through buffer exchange is not required, which prevents the otherwise unavoidable loss and dilution of the protein samples. Moreover, since the detergent is not introduced until the last step, it reduces the amount of detergent used. This is especially true for NMR sample preparations where the use of deuterated detergents is necessary and they are generally very expensive. We are currently investigating the versatility of this method using other integral membrane proteins.

Feasibility of Structural Determination by Solution NMR. To conduct structural determination of any membrane protein by solution NMR, detergent screening to find the suitable membrane mimetic is an essential prerequisite. The suitability of a detergent micelle is determined by taking into account the protein solubility and stability along with the quality of the 2D HSQC NMR spectrum. The 2D HSQC spectrum correlates the amide proton and the corresponding nitrogen pair of each residue within a protein and provides a map of the fingerprint region. It also serves as a building block for a multitude of multidimensional NMR experiments upon which the resonance assignments and the determination of the 3D structure of a protein rest. Thus, obtaining high-quality, i.e., sufficiently resolved, HSQC spectra is imperative for structural characterization by solution NMR.

To find a suitable detergent for obtaining a homogeneous sample of the C-terminal domain of Stt3p, we screened six detergents. These include digitonin, which has been successfully used to extract and reconstitute the OT complex in microsomes (*55*); SDS and DPC, which are commonly used for solution NMR; and LDAO, DDM, and OG, some of the common detergents used for membrane protein crystallization. As expected, digitonin gave unresolvable HSQC spectra because of its large micelles (70 kDa). For the rest of the detergents except OG and SDS, the protein appeared to be oligomerized, leading to

poorly resolved spectra with broad linewidths and missing resonances. For OG, while it has a small micellar size (25 kDa), it seems that its short alkyl chain (C8) jeopardizes the protein conformational stability since the number of HSQC peaks is much higher than expected. In contrast, SDS micelles yielded an HSQC spectrum that was far superior in quality in comparison to those of the rest of the detergents that were screened in all aspects: number of resonances, signal-to-noise ratio, dispersion, linewidths, and uniformity of signal intensities. In fact, SDS has served as one of the most popular detergents for IMP studies (*56*) and has been widely used as a membrane mimetic for membrane protein structural and functional studies (*9*, *57*−*61*). The high-quality HSQC spectra along with the CD and fluorescence data suggest that the C-terminal domain of Stt3p in SDS micelles is well-folded, producing a homogeneous sample. These support the feasibility of conducting solution NMR-based structural studies.

In fact, the quality of the 2D HSQC spectrum is much better than what would be expected for such a large protein−detergent complex, implying a relatively slow relaxation rate. The ^{15}N T_1 and T_2 relaxation measurements show that the rotational correlation time for the C-terminal domain of Stt3p in SDS micelles is surprisingly short (~10 ns), a value expected for a 20 kDa protein tumbling isotropically in solution (data not shown). This, however, is consistent with the results reported by Krueger-Koplin et al. (*9*), who found that a survey of seven membrane proteins in different detergent micelles showed a rather short rotational correlation time ranging from 8 to 12 ns. According to these authors, this phenomenon can be attributed to the fluid property of detergents that allows rotation of the proteins within the confines of the micelle. In the case of the C-terminal domain of Stt3p, an alternative explanation is its flexible dynamic property. The high flexibility of the C-terminal domain of Stt3p is reasonable since N-linked glycosylation is cotranslational. Therefore, only a flexible active site can recognize glycosylatable sequons rapidly and efficiently in all different types of growing polypeptide chains. This ensures the rapid discharge of the product from the active site. Furthermore, the flexibility of this domain is supported by the cryo-electron microscopy structure of the yeast OT, which shows a flexible groove formed between the lumenal domains of Ost1p, Wbp1p, and Stt3p (*62*). This groove is proposed to thread and scan the unfolded nascent polypeptide chain (*62*).

One striking feature of the C-terminal domain of Stt3p is that it is highly conserved in eukaryotes. Actually, the sequence alignment shows that, from yeast to humans, the sequence identity is > 50% (*10*). The strictly conserved "WWDYG" motif is believed to be the catalytic and/or acceptor protein recognition site. The aspartate residue (Asp^{518}) of this conserved motif was thought to function solely as a catalytic base (*11*). However, it appears that the role of Asp^{518} is more than simply acting as a base in the catalysis since the D518E mutation results in a complete loss of enzyme activity, even though both Asp and Glu residues have similarly charged side chains. If the role of Asp is just to act as a base, then how can the loss of activity for D518E be explained?

To address this question, we conducted comprehensive biophysical characterizations of the D518E mutant and wild-type C-terminal domain of Stt3p. Interestingly, while both the wild type and D518E mutant share nearly identical secondary structural contents, they have distinctly different tertiary structures as revealed by near-UV CD, fluorescence, and NMR spectroscopies. The most direct evidence for this conclusion has come from the comparison of their 2D HSQC spectra. The replacement of Asp^{518} with the longer Glu side chain leads to large global changes in the structure involving nearly all of the amino acid residues (Figure 8). This observation led to the conclusion that Asp^{518} is critical for the maintenance of the catalytically active conformational geometry of the C-terminal domain of Stt3p.

Additionally, the apparent disruption of the active conformation after a point mutation strongly suggests that the C-terminal domain of Stt3p has folded into its native conformation in SDS micelles. This is based on the fact that it is very unlikely to change the "structure" of a protein that is denatured or in a molten globule state by the replacement of one residue with a structurally similar residue.

The loss of enzyme activity *via* the mutation of Asp to Glu is not that common, but OT is not unique in this regard (*10*). In fact, for the enzyme Ca^{2+}-ATPase, D601E and D707E mutations result in an inactive enzyme (*63*). More importantly, residues Asp^{601} and Asp^{707} have been proposed to play structural but not catalytic or substrate recognition roles. It is therefore likely that OT and ATPase may have similar mechanisms of function.

In Vitro Functional Probing of the C-Terminal Domain of Stt3p. In this study, STD NMR and HSQC titrations were conducted to probe the *in vitro* protein−substrate interaction. Our results demonstrate that the C-terminal domain of Stt3p interacts with the acceptor peptide substrate containing the N-linked glycosylation recognition motif. The strong signals that belong exclusively to the acceptor peptide were observed in the STD spectrum, while chemical shift perturbations were observed in the HSQC experiments upon addition of the substrate peptide. These observations provide direct experimental proof that the C-terminal domain of Stt3p contains the recognition site for the N-glycosylation acceptor substrate even though the affinity is relatively low (K_D ~ 10 mM). One explanation could be that SDS micelles may not mimic the native lipid bilayer, which may impair the activity of the protein to some extent. Additionally, since the functional OT complex is composed of eight different subunits, it is more likely that while the C-terminal domain of Stt3p possesses the substrate recognition site, the other subunit(s) may facilitate the binding process (*62*).

The C-terminal domain of Stt3p in SDS micelles has a short rotational correlation time of ~10 ns, suggesting that it is a monomer under the experimental conditions. However, the sigmoidal saturation curve observed upon acceptor substrate binding indicates that this monomeric protein is allosterically activated, suggesting that it may contain more than one binding site. The binding of a peptide substrate (allosteric activator) to the activator site results in an increased affinity in the second site (active site). The detailed regulatory mechanism can be addressed only by further structure−function studies.

CONCLUSION

We have reported the overexpression of the C-terminal domain of the Stt3p subunit from the yeast *S. cerevisiae*. A robust, novel yet simple purification protocol called SDS elution has been developed. It is likely that this novel purification method may work for the purification and reconstitution of other recombinant integral membrane proteins. Far-UV CD data show C-terminal Stt3p is highly helical, while near-UV CD, fluorescence, and NMR experiments demonstrate the presence of a stable tertiary structure. In addition, our biophysical data suggest that the critical Asp^{518} residue plays a structural role in maintaining the strict conformational geometry necessary for the

catalytic activity of the enzyme. Our acceptor substrate binding studies indicate that this C-terminal Stt3p domain contains the acceptor peptide recognition site. The high-resolution 3D structure determinations of C-terminal Stt3p by both solution NMR and X-ray crystallography methods are well underway in our laboratory. The high-resolution structure will be instrumental in our understanding of the structure−function relationship and mechanisms of catalysis for this enzyme complex.

ACKNOWLEDGMENT

We are grateful to Prof. William J. Lennarz (distinguished professor at Stony Brook University, Stony Brook, NY) for the original Stt3p clone in yeast. We acknowledge Dr. David Zoetewey for critical reading of the manuscript.

REFERENCES

1. Knauer, R., and Lehle, L. (1999) The Oligosaccharyltransferase Complex from *Saccharomyces cerevisiae*. *Biochim. Biophys. Acta 1426*, 259–273.
2. Silberstein, S., and Gilmore, R. (1996) Biochemistry, molecular biology, and genetics of the oligosaccharyltransferase. *FASEB J. 10*, 849–858.
3. Welply, J. K., Shenbagamurthi, P., Lennarz, W. J., and Naider, F. (1983) Substrate recognition by oligosaccharyltransferase. Studies on glycosylation of modified Asn-X-Thr/Ser tripeptides. *J. Biol. Chem. 258*, 11856–11863.
4. Dempski, R. E., Jr., and Imperiali, B. (2002) Oligosaccharyl transferase: Gatekeeper to the secretory pathway. *Curr. Opin. Chem. Biol. 6*, 844–850.
5. Helenius, A., and Aebi, M. (2004) Roles of N-linked glycans in the endoplasmic reticulum. *Annu. Rev. Biochem. 73*, 1019–1049.
6. Marquardt, T., and Denecke, J. (2003) Congenital disorders of glycosylation: Review of their molecular bases, clinical presentations and specific therapies. *Eur. J. Pediatr. 162*, 359–379.
7. Zubkov, S., Lennarz, W. J., and Mohanty, S. (2004) Structural basis for the function of a minimembrane protein subunit of yeast oligosaccharyltransferase. *Proc. Natl. Acad. Sci. U.S.A. 10*, 3821–3826.
8. Igura, M., Maita, N., Kamishikiryo, J., Yamada, M., Obita1, T., Maenaka, K., and Kohda, D. (2008) Structure-guided identification of a new catalytic motif of oligosaccharyltransferase. *EMBO J. 27*, 234–243.
9. Krueger-Koplin, R., Sorgen, P., Krueger-Koplin, S., Rivera-Torres, I., Cahill, S., Hicks, D., Grinius, L., Krulwich, T., and Girvin, M. (2004) An evaluation of detergents for NMR structural studies of membrane proteins. *J. Biomol. NMR 28*, 43–57.
10. Zufferey, R., Knauer, R., Burda, P., Stagljar, I., te Heesen, S., Lehle, L., and Aebi, M. (1995) STT3, a highly conserved protein required for yeast oligosaccharyl transferase activity *in vivo*. *EMBO J. 14*, 4949–4960.
11. Yan, Q., and Lennarz, W. J. (2002) Studies on the Function of Oligosaccharyl Transferase Subunits. *J. Biol. Chem. 277*, 47692–47700.
12. Kelleher, D. J., Karaoglu, D., Mandon, E. C., and Gilmore, R. (2003) Oligosaccharyltransferase isoforms that contain different catalytic STT3 subunits have distinct enzymatic properties. *Mol. Cell 12*, 101–111.
13. Nilsson, I., Kelleher, D. J., Miao, Y., Shao, Y., Kreibich, G., Gilmore, R., von Heijne, G., and Johnson, A. E. (2003) Photocross-linking of nascent chains to the STT3 subunit of the oligosaccharyltransferase complex. *J. Cell Biol. 161*, 715–725.
14. Glover, K. J., Weerapana, E., Numao, S., and Imperiali, B. (2005) Chemoenzymatic Synthesis of Glycopeptides with PglB, a Bacterial Oligosaccharyl Transferase from *Campylobacter jejuni*. *Chem. Biol. 12*, 1311–1315.
15. Feldman, M. F., Wacker, M., Hernandez, M., Hitchen, P. G., Marolda, C. L., Kowarik, M., Morris, H. R., Dell, A., Valvano, M. A., and Aebi, M. (2005) Engineering N-linked protein glycosylation with diverse O antigen lipopolysaccharide structures in *Escherichia coli*. *Proc. Natl. Acad. Sci. U.S.A. 102*, 3016–3021.
16. Nasab, F. P., Schulz, B. L., Gamarro, F., Parodi, A. J., and Aebi, M. (2008) All in One: *Leishmania major* STT3 Proteins Substitute for the Whole Oligosaccharyltransferase Complex in *Saccharomyces cerevisiae*. *Mol. Biol. Cell 19*, 3758–3768.
17. Hese, K., Otto, C., Routier, F. H., and Lehle, L. (2009) The yeast oligosaccharyltransferase complex can be replaced by STT3 from *Leishmania major*. *Glycobiology 19*, 160–171.
18. Kim, H., von Heijne, G., and Nilsson, I. (2005) Membrane Topology of the STT3 Subunit of the Oligosaccharyl Transferase Complex. *J. Biol. Chem. 280*, 20261–20267.
19. Cserzö, M., Wallin, E., Simon, I., von Heijne, G., and Elofsson, A. (1997) Prediction of transmembrane α-helices in procariotic membrane proteins: The Dense Alignment Surface method. *Protein Eng. 10*, 673–676.
20. von Heijne, G. (1992) Membrane protein structure prediction. *J. Mol. Biol. 225*, 487–494.
21. Hofmann, K., and Stoffel, W. (1993) TMBASE: A database of membrane spanning protein segments. *Biol. Chem. Hoppe-Seyler 374*, 166.
22. Juretic, D., Zoranic, L., and Zucic, D. (2002) Basic charge clusters and predictions of membrane protein topology. *J. Chem. Inf. Comput. Sci. 42*, 620–632.
23. Pace, C. N., Vajdos, F., Fee, L., Grimsley, G., and Gray, T. (1995) How to measure and predict the molar absorption coefficient of a protein. *Protein Sci. 4*, 2411–2423.
24. Delaglio, F., Grzesiek, S., Vuister, G. W., Zhu, G., Pfeifer, J., and Bax, A. (1995) NMRPipe: A multidimensional spectral processing system based on UNIX pipes. *J. Biomol. NMR 6*, 277–293.
25. Rosinke, B., Strupat, K., Hillenkamp, F., Rosenbusch, J., Dencher, N., Kruger, U., and Galla, H. (1995) Matrix-assisted laser desorption/ionization mass spectrometry (MALDI-MS) of membrane proteins and non-covalent complexes. *J. Mass Spectrom. 30*, 1462–1468.
26. Galvani, M., and Hamdan, M. (2000) Electroelution and passive elution of γ-globulins from sodium dodecyl sulphate polyacrylamide gel electrophoresis gels for matrix-assisted laser desorption/ionisation time-of-flight mass spectrometry. *Rapid Commun. Mass Spectrom. 14*, 721–723.
27. Jeannot, M. A., Jing, Z., and Li, L. (1999) Observation of sodium gel-induced protein modifications in dodecylsulfate polyacrylamide gel electrophoresis and its implications for accurate molecular weight determination of gel-separated proteins by matrix-assisted laser desorption ionization time-of-flight mass spectrometry. *J. Am. Soc. Mass Spectrom. 1999* (10), 512–520.
28. Gasteiger, E., Gattiker, A., Hoogland, C., Ivanyi, I., Appel, R. D., and Bairoch, A. (2003) ExPASy: The proteomics server for in-depth protein knowledge and analysis. *Nucleic Acids Res. 31*, 3784–3788.
29. Chatterjee, S., Schoepe, J., Lohmer, S., and Schomburg, D. (2005) High level expression and single-step purification of hexahistidine-tagged L-2-hydroxyisocaproate dehydrogenase making use of a versatile expression vector set. *Protein Expression Purif. 39*, 137–143.
30. Page, R. C., Moore, J. D., Nguyen, H. B., Sharma, M., Chase, R., Gao, F. P., Mobley, C. K., Sanders, C. R., Ma, L., Sönnichsen, F. D., Lee, S., Howell, S. C., Opella, S. J., and Cross, T. A. (2006) Comprehensive evaluation of solution nuclear magnetic resonance spectroscopy sample preparation for helical integral membrane proteins. *J. Struct. Funct. Genomics 7*, 51–64.
31. Batenjany, M. M., Mizukami, H., and Salhany, J. M. (1993) Near-UV circular dichroism of band 3. Evidence for intradomain conformational changes and interdomain interactions. *Biochemistry 32*, 663–668.
32. Taylor, R. M., Zakharov, S. D., Bernard, H. J., Girvin, M. E., and Cramer, W. A. (2000) Folded state of the integral membrane colicin E1 immunity protein in solvents of mixed polarity. *Biochemistry 39*, 12131–12139.
33. Turk, E., Gasymov, O. K., Lanza, S., Horwitz, J., and Wright, E. M. (2006) A reinvestigation of the secondary structure of functionally active vSGLT, the *Vibrio* sodium/galactose cotransporter. *Biochemistry 45*, 1470–1479.
34. Demarest, S. J., Boice, J. A., Fairman, R., and Raleigh, D. P. (1999) Defining the core structure of the α-lactalbumin molten globule state. *J. Mol. Biol. 294*, 213–221.
35. Ladokhin, A. S., Jaysainghe, S., and White, S. H. (2000) How to Measure and Analyze Tryptophan Fluorescence in Membranes Properly, and Why Bother? *Anal. Biochem. 285*, 235–245.
36. Reshetnyak, Y. K., Koshevnik, Y., and Burstein, E. A. (2001) Decomposition of Protein Tryptophan Fluorescence Spectra into Log-Normal Components. III. Correlation between Fluorescence and Microenvironment Parameters of Individual Tryptophan Residues. *Biophys. J. 81*, 1735–1758.
37. Reithmeier, R. A. (1995) Characterization and modeling of membrane sequence analysis. *Curr. Opin. Struct. Biol. 5*, 491–500.
38. Deber, C. M., and Goto, N. K. (1996) Folding proteins into membranes. *Nat. Struct. Biol. 3*, 815–818.

39. Landolt-Marticorena, C., Williams, K. A., Deber, C. M., and Reithmeier, R. A. (1993) Non-random distribution of amino acids in the transmemrbane segments of human type I single span membrane proteins. *J. Mol. Biol. 229*, 602–608.
40. Eftink, M. R. (1991) Methods of Biochemical Analysis, pp 127−205, John Wiley, New York.
41. Lakowicz, J. R. (1999) Principles of Fluorescence Spectroscopy, Kluwer-Plenum, New York.
42. Vivian, J. T., and Callis, P. R. (2001) Mechanisms of Tryptophan Fluorescence Shifts in Protein. *Biophys. J. 80*, 2093–2109.
43. Mayer, M., and Meyer, B. (1999) Characterization of ligand binding by saturation transfer difference NMR spectroscopy. *Angew. Chem., Int. Ed. 38*, 1784–1788.
44. Mayer, M., and Meyer, B. (2001) Group epitope mapping by saturation transfer difference NMR to identify segments of a ligand in direct contact with a protein receptor. *J. Am. Chem. Soc. 123*, 6108–6117.
45. Peng, J. W., Lepre, C. A., Fejzo, J., Abdul-Manan, N., and Moore, J. M. (2001) Nuclear magnetic resonance-based approaches for lead generation in drug discovery. *Methods Enzymol. 338*, 202–230.
46. Stockman, B. J., and Dalvit, C. (2002) NMR screening techniques in drug discovery and drug design. *Prog. Nucl. Magn. Reson. Spectrosc. 41*, 187–231.
47. Meinecke, R., and Meyer, B. (2001) Determination of the binding specificity of an integral membrane protein by saturation transfer difference NMR: RGD peptide ligands binding to integrin $\alpha_{IIb}\beta_3$. *J. Med. Chem. 44*, 3059–3065.
48. Streiff, J. H., Juranic, N. O., Macura, S. I., Warner, D. O., Jones, K. A., and Perkins, W. J. (2004) Saturation Transfer Difference Nuclear Magnetic Resonance Spectroscopy as a Method for Screening Proteins for Anesthetic Binding. *Mol. Pharmacol. 66*, 929–935.
49. Tugarinov, V., and Kay, L. E. (2003) Ile, Leu, and Val methyl assignments of the 723-residue malate synthase G using a new labeling strategy and novel NMR methods. *J. Am. Chem. Soc. 125*, 13868–13878.
50. Tate, C. G. (2001) Overexpression of mammalian integral membrane proteins for structural studies. *FEBS Lett. 504*, 94–98.
51. Mayumi, I., Nobuo, M., Obita, T., Kamishikiryo, J., Maenaka, K., and Kohda, D. (2007) Purification, crystallization and the preliminary X-ray diffraction studies of the soluble domain of the oligosaccharyltransferase STT3 subunit from the thermophilic archaeon *Pyrococcus furiosus*. *Acta Crystallogr. F63*, 798–801.
52. Rogl, H., Kosemund, K., Kuhlbrandt, W., and Collinson, I. (1998) Refolding of *Escherichia coli* produced membrane protein inclusion bodies immobilised by nickel chelating chromatography. *FEBS Lett. 432*, 21–26.
53. Gorzelle, B. M., Nagy, J. K., Oxenoid, K., Lonzer, W. L., Cafiso, D. S., and Sanders, C. R. (1999) Reconstitutive refolding of diacylglycerol kinase, an integral membrane protein. *Biochemistry 38*, 16373–16382.
54. Baneres, J. L., Martin, A., Hullot, P., Girard, J. P., Rossi, J. C., and Parello, J. (2003) Structure-based Analysis of GPCR Function: Conformational Adaptation of both Agonist and Receptor upon Leukotriene B_4 Binding to Recombinant BLT1. *J. Mol. Biol. 329*, 801–814.
55. Kelleher, D. J., Kreibich, G., and Gilmore, R. (1992) Oligosaccharyltransferase activity is associated with a protein complex composed of ribophorins I and II and a 48 kD protein. *Cell 69*, 55–65.
56. Baleja, J. D. (2001) Structure determination of membrane-associated proteins from NMR data. *Anal. Biochem. 288*, 1–15.
57. Chill, J. H., Louis, J. M., Miller, C., and Bax, A. (2006) NMR study of the tetrameric KcsA potassium channel in detergent micelles. *Protein Sci. 15*, 684–698.
58. Jaroniec, C. P., Kaufman, J. D., Stahl, S. J., Viard, M., Blumenthal, R., Wingfield, P. T., and Bax, A. (2005) Structure and Dynamics of Micelle-Associated Human Immunodeficiency Virus gp41 Fusion Domain. *Biochemistry 44*, 16167–16180.
59. Howell, S. C., Mesleh, M. F., and Opella, S. J. (2005) NMR Structure Determination of a Membrane Protein with Two Transmembrane Helices in Micelles: MerF of the Bacterial Mercury Detoxification System. *Biochemistry 44*, 5196–5206.
60. Lee, S., Mesleh, M. F., and Opella, S. J. (2003) Structure and dynamics of a membrane protein in micelles from three solution NMR experiments. *J. Biomol. NMR 26*, 327–334.
61. Mascioni, A., Porcelli, F., Ilangovan, U., Ramamoorthy, A., and Veglia, G. (2003) Conformational preferences of the amylin nucleation site in SDS micelles: An NMR study. *Biopolymers 69*, 29–41.
62. Li, H., Chavan, M., Schindelin, H., Lennarz, W. J., and Li, H. (2008) Structure of the Oligosaccharyl Transferase Complex at 12 Å Resolution. *Structure 16*, 432–440.
63. Clarke, D. M., Loo, T. W., and MacLennan, D. H. (1990) Functional consequences of alterations to amino acids located in the nucleotide binding domain of the Ca^{2+}-ATPase of sarcoplasmic reticulum. *J. Biol. Chem. 265*, 22223–22227.